Title
Flow Evaporimeter To Assess Evaporative Resistance of Human Tear-Film Lipid Layer

Journal
Industrial & Engineering Chemistry Research, 53(47)

ISSN
0888-5885

Authors
Peng, C-C
Cerretani, C
Li, Y
et al.

Publication Date
2014-11-26

DOI
10.1021/ie5030497

Peer reviewed

I&EC research
Industrial & Engineering Chemistry Research

Article

pubs.acs.org/IECR

Flow Evaporimeter To Assess Evaporative Resistance of Human Tear-Film Lipid Layer

C.-C. Peng,[†] C. Cerretani,[†] Y. Li,[†] S. Bowers,[†] S. Shahsavarani,[†] M. C. Lin,[‡,§] and C. J. Radke*[,†,§]

[†]Department of Chemical and Biomolecular Engineering, [‡]Clinical Research Center, School of Optometry, and [§]Vision Science Graduate Program, University of California, Berkeley, California 94720, United States

ABSTRACT: A novel in vivo flow evaporimeter is developed to measure human tear-evaporation rates. The flow evaporimeter relies on a well-defined flow field to the eye with known and adjustable flow rates and relative humidities, and quantitatively reproduces evaporation rates for pure water. Mass-transfer analysis of the evaporimeter data elucidates, for the first time, the resistance of the human tear-film lipid layer (TFLL) toward minimizing tear loss to the environment. A pilot study on human subjects validates the feasibility of the flow evaporimeter to obtain the tear-film evaporation rates in vivo. Resistance of the TFLL against tear evaporation is found subject specific. Our flow evaporimeter offers an accurate, safe, and convenient diagnostic tool for clinical evaluation of dry-eye-related maladies.

1. INTRODUCTION

Dry-eye disease is one of the most frequently encountered human ocular disorders. It afflicts up to 60% of the world's population, depending on geographic region,[1−6] and is exacerbated by dry climates and by aging.[7−10] There are approximately 4 million dry-eye sufferers in the United States alone.[6,11−13] Symptoms of dry eye are reported by 25% of patients who visit ophthalmic clinics.[14]

A primary cause of dry eye is excessive evaporation of the aqueous of tears.[15] As tear aqueous evaporates, salinity increases.[16,17] At elevated evaporation rates, increased salinity stimulates afferent corneal epithelial nerves, thereby signaling irritating dry-eye symptoms.[15,18−20] The human tear film, deposited during each blink at approximately 5 μm thick,[21−23] consists mainly of dilute proteins, salts, and mucins.[24] A thin 100 nm tear-film lipid layer (TFLL) coats the anterior surface of the tear.[25,26] It is thought to function as a barrier against aqueous evaporation.[27−29] In fact, with an unstable[30−33] or insufficient TFLL, evaporation can be sufficient to irritate and, for some patients, damage the corneal epithelial cell layer.

Clearly, tear-evaporation rate provides a key to understand and possibly alleviate dry eye. Recently, several helpful mathematical models of tear-evaporation dynamics[16,17,33] and in vitro experiments[34] have been established. Unfortunately, these results are insufficient to validate evaporation rates from human tears.[34] Indeed, because of the paramount importance of tear evaporation to anterior-eye health, and also to comfortable contact-lens wear,[35] considerable effort has been expended on measuring tear-evaporation rates in vivo.[27,36−59]

Two basic in vivo evaporimeter designs are available: those with closed chambers and those with open chambers. Both chamber types are attached to closed goggles to protect against direct eye contact. In a closed-chamber design, relative humidity is detected a set distance away from the eye as a function of time while the chamber accumulates water vapor. These devices include those of Rolando and Refojo,[37] Tsubota and Yamada,[42] Mathers,[44] and Rohit et al.[55,57] Most reported measurements in closed chambers are with the Mathers' evaporimeter (Oxdata, Portland, OR, USA).[43−46,49−54] In a closed cylinder affixed perpendicularly to a goggle face, the humidity rises as tear evaporates. However, air in the chamber is not completely stagnant due to eye saccades and to lid-blink motion causing the surrounding air to circulate. Accordingly, diffusion is not dominant. In addition, circulation strength is insufficient to mix the surrounding air in the chamber completely, leading to nonuniformly distributed water-vapor concentration in the chamber. Data-interpretation schemes for all closed-chamber instruments assume that the air is well-mixed in the goggle and, accordingly, lead to error. In addition, air temperature in the closed chamber is not uniform, so the values of measured relative humidity are questionable.

Evaporimeters open to the environment fall into two classes: those with imposed air flow and those without. Tomlinson and Trees[39] utilized a cylinder open to the environment but with no flow (Servo Med, EP1, Stockholm, Sweden). Two humidity detectors were placed a known distance apart along the axis of the cylinder. Tear-evaporation rate at steady state was ascertained by assuming molecular diffusion between the two detectors. Khanal et al.[60] later used the Servo-Med evaporimeter to study tear evaporation rates on both dry-eye and normal subjects. With this instrument, they determined a threshold tear-evaporation rate of 9.2×10^{-7} g/cm^2/s (33 g/m^{-2}/h) for dry eye.[60] To our knowledge, this is the only evaporimetric diagnosis for dry eye reported in the literature.[61] The major drawback of the Servo-Med instrument, as noted above, is that air is not stagnant in the chamber attached to the eye, invalidating diffusion-based data interpretation. Further, because the chamber is partially open to the environment, changes in environment lead to differing and uncontrolled results unless a complete environmental chamber is used.[10,54]

Apparently, Cedarstaff and Tomlinson[56] were the first to employ a goggle evaporimeter with imposed flow. Their

Received: July 30, 2014
Revised: November 2, 2014
Accepted: November 3, 2014
Published: November 3, 2014

dx.doi.org/10.1021/ie5030497 | Ind. Eng. Chem. Res. 2014, 53, 18130−18139

instrument supplied air humidified to 70% and parallel to contact-lens-covered eyes. These authors do not vary the air flow rate. Later, Goto et al.[48] also employed a flow evaporimeter. In their instrument, dry air flows normal into a goggle and egresses separately through a cylinder affixed to the goggle face and containing an oscillating quartz crystal to detect exit humidity. Strictly, this instrument gives an evaporation rate at zero relative humidity, which is an extremely harsh environment to the eye. Hereto, no provision was made to alter the inlet flow rate to the eye, which surely changes the evaporation rate.

Other instruments have been employed to detect tear evaporation rates indirectly including transient tear thickness from interferometry[31,32] and transient ocular temperature from IR thermography.[58,59] As opposed to evaporimeters, both methods detect local evaporation rates and must be averaged. Neither methodology considers the important roles of environment humidity, air flow, and temperature.

Mathers reviews results from the various instruments, many of them contradictory.[50] Unfortunately, he does not elucidate the deficiencies of the various instrument designs. Tear-evaporation rate still remains rarely examined during clinical diagnosis. To provide meaningful measurement of in vivo tear-evaporation rate, an evaporimeter must provide

(1) a well-defined flow field to the eye with known and adjustable flow rates, relative humidities, and temperatures
(2) repeatable and accurate evaporation-rate measurements for pure water, closely matching documented values for defined relative humidities and flow rates[34]

Only a flow evaporimeter meets the stated criteria. The need for air flow is threefold. First, flow is essential because establishing completely stagnant conditions in a chamber is not possible. Second, tear evaporation into the environment exposes the eye to air flow, as in walking and running, to air conditioning, to forced-air heating, etc. Even during sitting, the human eye is exposed to air currents. Third, and most importantly, a well-defined flow field is necessary to characterize the mass-transfer behavior of the instrument. Without such characterization, it is not possible to assess the TFLL evaporation resistance, the major deterrent to tear evaporation. To understand tear evaporation, air flow is requisite.[34]

No currently available evaporimeter has the features cited as necessary to obtain valid tear-evaporation rates and quantitative evaporation resistances of the TFLL on humans. This means that all results obtained to date on, for example, the importance of tear evaporation in dry eye, meibomian-gland disease,[62,63] tear-salinity control,[16,17,33] contact-lens wear,[35,52,57,64] and topical drug delivery[65,66] are suspect and in need of reexamination. For these reasons, we design an accurate, safe, and convenient flow evaporimeter that meets the stated design criteria and is suitable for clinical evaluation of dry-eye-related maladies. Because the flow evaporimeter supplies its own environment (i.e., air flow, temperature, and humidity), there is no need for an expensive environmental chamber.

2. EVAPORIMETER DESIGN

2.1. Tear-Evaporation Physics. Figure 1 illustrates that, when a duplex lipid layer covers the tear film, water molecules (small filled circles) first dissolve in the lipid, diffuse across the lipid layer, and then evaporate into the air environment (large open circles).[34] Two resistances to evaporation appear: one for

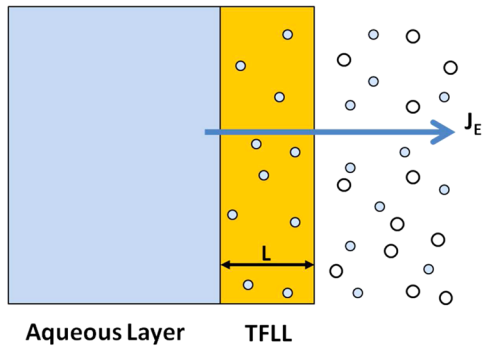

Figure 1. Schematic of dissolution/evaporation mechanism. Water molecules (small filled circles) dissolve in the tear-film lipid layer (TFLL) of thickness L and subsequently evaporate into air (large open circles). Evaporation flux is labeled as J_E.

transporting water across the TFLL, R_L, and one for transporting the water molecules into the air, R_m, the gas-phase mass-transfer resistance.[34,67] Following dissolution into the lipid layer, water evaporation occurs by liquid water molecules gaining sufficient energy to overcome the attractive forces of nearby lipid molecules and escaping from the air/lipid surface as water vapor. Hindrance from the environmental air molecules, however, slows molecular evaporation.

Evaporative water flux in Figure 1 obeys the following linear expression:[34,67]

$$J_E = (R_L + R_m)^{-1}[C_{sat}(T_S) - C_\infty(T_\infty)] = (R_L + R_m)^{-1}[C_{sat}(T_S) - R_H C_{sat}(T_\infty)] \quad (1)$$

where J_E is the evaporation rate (flux) in g/cm^2/s, C_{sat} is the saturation concentration of water vapor in the air at temperature T, C_∞ is the concentration of water vapor in the air far from the evaporating surface, T_S is the temperature of the evaporating eye surface, and T_∞ is the temperature of the environment far from the eye. Resistances of the lipid layer and the air environment are in series and, hence, additive. The relative humidity of the environment, R_H, appears in the far right of eq 1 and indicates that the evaporation rate changes with relative humidity. This explains the important role of humidity in eye comfort. For example, it is well-known that dry-eye discomfort disappears during goggle wear.[31,68] When the air in the goggles saturates with water vapor ($R_H = 1$), tear evaporation effectively ceases.

Human tear evaporation follows a periodic steady state imposed by the blink process (i.e., repetition of a 0.2-s blink followed by a 5-s open-eye interblink). Equation 1, however, strictly applies at steady state. Fortunately, the periodic temperature excursions of the anterior eye surface are minimal;[33,69,70] evaporation rate is, thus, unaffected.

Although the resistance of the TFLL to tear evaporation, R_L, depends on film thickness, lipid affinity to water molecules, and possibly other lipid physicochemical properties such as viscosity and elasticity,[34] it remains unclear how the human TFLL retards tear evaporation in vivo due to the limitation of available and reliable studies. Apparently, no in vitro model can perfectly reproduce in vivo results.[34] To discern the role of the TFLL (i.e., R_L) in the etiology of dry eye, a quantitative measure of in vivo tear evaporation is essential.

Both environment mass-transfer and TFLL evaporative resistances appear in eq 1. To establish each, we recognize that the environmental mass-transfer resistance of a flow

dx.doi.org/10.1021/ie5030497 | Ind. Eng. Chem. Res. 2014, 53, 18130−18139

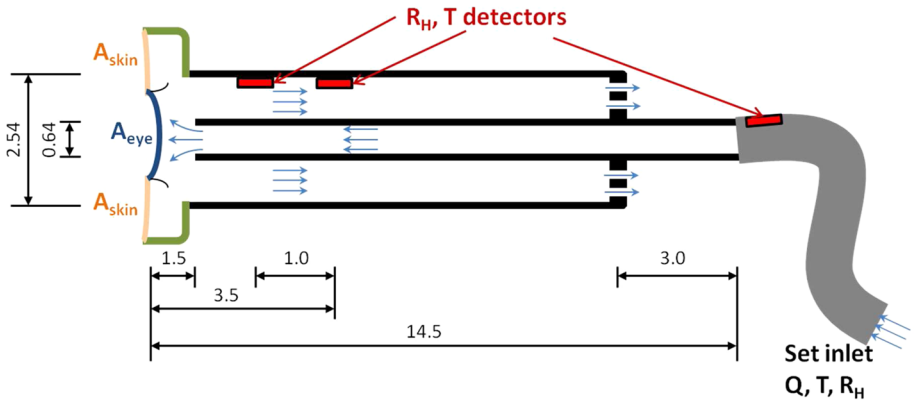

Figure 2. Schematic of proposed flow evaporimeter attached to a goggle. At a set flow volumetric rate, Q, inlet and exit relative humidities, R_H, and temperatures, T, are measured permitting calculation of evaporation rate. Dimensions are in centimeters. Drawing is not drawn to scale.

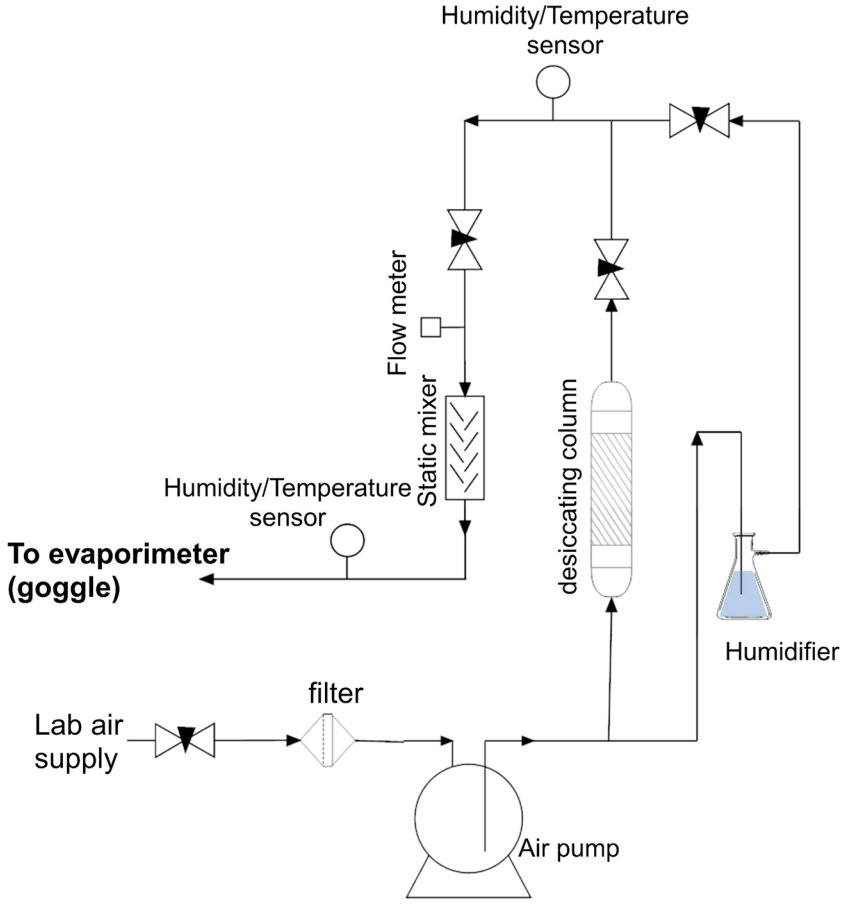

Figure 3. Schematic of the flow-evaporimeter humidification system.

evaporimeter, R_m, scales inversely as the air-flow velocity, v, to a noninteger power, β:[67]

$$R_m \sim v^{-\beta} \tag{2}$$

Thus, eq 1 can be rewritten as[71]

$$\frac{\Delta C}{J_E} = R_L + R_m = R_L + \alpha v^{-\beta} \tag{3}$$

where $\Delta C \equiv C_{sat}(T_S) - R_H C_{sat}(T_\infty)$ and α and β are constants characteristic of the evaporimeter flow field. Provided the flow evaporimeter obeys eq 3 with an evaporative resistance of the TFLL independent of flow velocity, measurement of $\Delta C/J_E$ as a function of air velocity to the negative β power for differing relative humidities yields a straight line independent of relative humidity.[71] The slope of that line depends only on the instrument, independent of the human subject. The intercept specifies the resistance of the TFLL which in the dissolution/diffusion picture of Figure 1 is given by

$$R_L = L/Dk \tag{4}$$

where L is the average thickness of the TFLL, D is the diffusivity of water in the TFLL, and k is the partition coefficient of water dissolved in the lipid layer.[34] R_L is a

dx.doi.org/10.1021/ie5030497 | Ind. Eng. Chem. Res. 2014, 53, 18130−18139

physiologic parameter of each human subject based on the TFLL thickness and lipid composition.

2.2. Flow Evaporimeter. Figure 2 illustrates the flow evaporimeter. The outer Plexiglas cylinder of the evaporimeter is attached perpendicularly to the right face of a sealed swim goggle (Speedo Vanquisher Optical Goggle 7500482, Sydney, Australia). A perforated 2 cm thick Teflon annular disk press fits the inner cylinder concentrically to the outer cylinder. The eye end of the inner cylinder is elevated about 1.5 cm away from the eye surface. The lengths/inner diameters of the outer and inner cylinders are 10/2.54 cm and 13/0.64 cm, respectively. Air of known relative humidity (humidity/temperature sensor, SHT75, Sensirion, Stäfa, Switzerland), temperature (humidity/temperature sensor, SHT75, Sensirion, Stäfa, Switzerland), and volumetric flow rate (electronic flow meter, ASF1400, Sensirion, Stäfa, Switzerland) is fed through the inner cylinder in impinging flow[72−74] onto the eye. Incoming air moistens by tear evaporation and exits through the outer cylinder. Exit air temperature and relative humidity are measured capacitively by the average readings from two Sensirion humidity/temperature sensors affixed to the outer cylinder approximately 1 and 2 cm downstream from the entrance to the outer cylinder. Exit air humidity and temperature prove insensitive to small changes in the positions of the probes. As illustrated in Figure 2, inlet relative humidity is measured by a third humidity probe located at the flow inlet.

Figure 3 shows that air humidity and flow rate to the evaporimeter are set by mixing dry air with water-saturated air. Laboratory air is filtered and pumped (Aquarium Air Pump, Rena Air 300, Gütenbach, Germany) to a 1-L fritted-glass water sparger for humidification and to a 10 cm long, 3 cm diameter desiccating column containing indicating Drierite (W. A. Hammond Drierite Co., Xenia, OH, USA). Water-saturated and dry-air flows are adjusted by two downstream 1 cm diameter Swagelok needle valves (Swagelok Northern California, Fremont, CA, USA). Following humidity/temperature and flow measurement, evaporimeter air supply is further mixed by passing through a 10 cm long, 2 cm diameter inline static mixer (Kenics-KM 12-element static mixer, Chemineer, Dayton, OH, USA). The air-supply flow is finely adjusted by the needle valve of the electronic flow meter and is maintained gentle to the eye (typical Reynolds numbers in the inner tube of the evaporimeter are between 20 and 80 characteristic of laminar flow). Data are automatically collected on a computer and analyzed with in-house implementation of available software (Labview 7.0, National Instruments, Austin, TX, USA).

Mass conservation at steady state establishes the tear-evaporation rate from the measured increase in exit relative humidity, R_{He}, over that of the inlet air stream, R_{Hi}:

$$JA = \frac{QM_w}{R_g}\left[\frac{R_{He}P_{sat}(T_e)}{T_e} - \frac{R_{Hi}P_{sat}(T_i)}{T_i}\right] \quad (5)$$

where J is the mass-evaporative flux from the skin and eye surfaces exposed in the goggle of total evaporation area A, Q is the air volumetric flow rate, M_w is the molecular weight of water, R_g is the ideal gas constant, and P_{sat} is the vapor pressure of water at absolute temperature, T. Thus, the precision of the evaporimeter depends on the precision of the relative-humidity probes. The evaporation rate in eq 5 includes evaporation from both exposed skin and eye. Following others,[38,60,75] we measure evaporation with the eye open and closed to correct for the contribution of water evaporation from exposed skin

$$J_E A_E = (JA)_{open} - (JA)_{closed}[A_{skin}/(A_{skin} + A_E)] \quad (6)$$

where $(JA)_{open}$ and $(JA)_{closed}$ are measured by the evaporimeter according to eq 5 for the open eye and closed eye, respectively. A_{skin} is the area of skin exposed during open-eye measurement, and A_E is the area of the eye palpebral fissure. In summary, the product JA is measured by the flow evaporimeter in closed and open eyes, human skin and eye areas are determined as described below, and the average evaporation rate from the tear film, J_E, is calculated following eq 6. Evaporation measurements are then taken as a function of relative humidity and air flow rate, satisfying criterion 1 (see section 1) for an acceptable evaporimeter.

2.3. Evaporimeter Validation. It is critical that the flow evaporimeter conform to eqs 1 and 2 by correctly measuring known evaporation rates for pure water, including the effects of flow and relative humidity (criterion 2; see section 1). This exercise gives independent assessment of the environmental air resistance, R_m, and its flow dependence, thereby allowing determination of TFLL resistance on human subjects (see eqs 3 and 4). To our knowledge, no current evaporimeter meets this criterion. To validate our instrument, the right side of an anatomically correct, realistic female mannequin head (MD-HelenF3, Roxy Display, Vernon, CA, USA) with additional eye lashes glued above and below the eyes was fitted with the flow evaporimeter. Prior to fitting, the right eye was excised and replaced by agar gel prepared by agarose powder (A9539 Sigma-Aldrich, Milwaukee, WI, USA) that evaporates at the same rate as that of pure water.[34,76] A 1 mL volume of oversaturated agarose solution (99.5 wt % prepared at 100 °C) was carefully injected into the carved space and shaped to mimic that of a human eye. The agarose gel subsequently set after reaching equilibrium with room temperature (~23 °C). The evaporating-surface temperature was monitored with a K-type thermocouple and digital thermometer (HH509R, Omega Engineering, Stamford, CT, USA). The evaporative area of the gelled-mannequin eye was measured following the same procedure as that for human eyes, described below. No correction was necessary for exposed skin area of the mannequin.

All evaporation measurements were performed in an air-conditioned room at constant temperature, i.e., $T_\infty \sim 23$ °C. For the mannequin-eye model, the agarose-gel anterior surface temperature during evaporation measured slightly less than but close to 23 °C. Thus, $T_S \sim 23$ °C for the mannequin eye. For human subjects, T_S was not directly measured. However, available calculations for the evaporating-tear surface temperature demonstrate minimal deviation from eye temperature.[33,69,70] Thus, T_S for humans was set to 35 °C independent of evaporation rate.

The goggle-wearing eye portion of the mannequin fitted with the flow evaporimeter was placed on an electronic balance (MS 304S, Mettler-Toledo, Columbus, OH, USA) with accuracy of ±0.1 mg. Thus, two simultaneous measurements of the pure-water evaporation rate are available: gravimetric and evaporimetric. Figure 4 compares evaporation rates on the mannequin eye from the evaporimeter and from weight loss for differing air flow rates between 2.5 and 22.5 cm/s at 3% inlet relative humidity. Exact agreement between the two measurements in Figure 4 is indicated by a straight line with unity slope. With a fixed unity slope, the best-fit intercept of the shown fitting line

dx.doi.org/10.1021/ie5030497 | Ind. Eng. Chem. Res. 2014, 53, 18130−18139

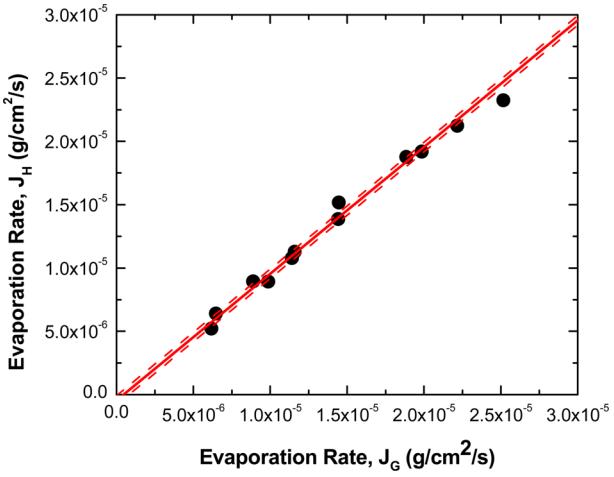

Figure 4. Pure-water evaporation flux (filled circles) from the mannequin eye measured by the flow evaporimeter, J_H, versus that measured gravimetrically, J_G, at 3% relative humidity and T_S = 23 °C. Inlet air flow rates were varied between 2.5 and 22.5 cm/s. The solid straight line is the linear-fit result with slope = 1. The intercept of the fitting line is $(-4.5 \pm 1.7) \times 10^{-7}$ g/cm^2/s. Dashed lines set the upper and lower boundaries of the 95% confidence interval.

is $(-4.5 \pm 1.7) \times 10^{-7}$ g/cm^2/s, indicating the detection limit and precision of our instrument. Inherent variability of the flow evaporimeter is about 1 order of magnitude smaller than previously reported human tear film evaporation rates.[50,77,78] Hence, criterion 2 is met by the new flow evaporimeter.

Figure 5 graphs the pure-water evaporation flux at ambient temperature from the mannequin gelled eye as a function of

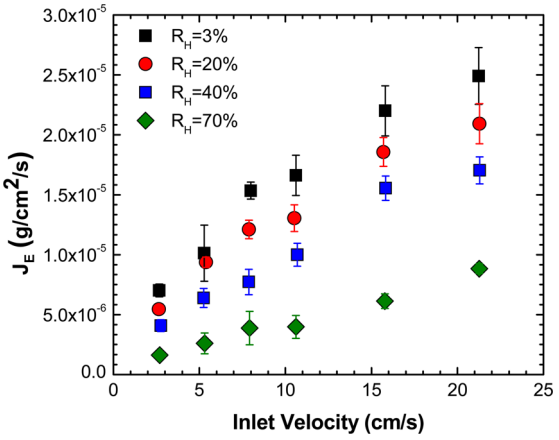

Figure 5. Evaporative flux at T_S = 23 °C as a function of velocity from the mannequin eye (pure water) for various relative humidities. Data are presented as mean ± standard deviation (SD) (n = 5).

evaporimeter air velocity for three different inlet relative humidities. Lower humidity and higher flow velocity increase evaporation rates, which is in agreement with eqs 1 and 3. These results are consistent with pure-water evaporation rates directly measured at various flow rates and relative humidities.[79,80]

Figure 6 replots the pure-water evaporation flux from the mannequin eye in Figure 5 but in terms of eq 3 for various inlet relative humidities. To determine the power index appearing in the abscissa, a log–log plot of $\Delta C/J_E$ versus v was first constructed; linear regression of the data yields β = 0.8. Figure

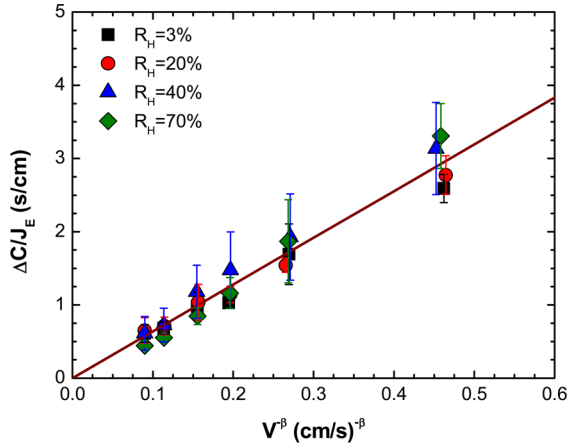

Figure 6. Evaporimeter-determined results at T_S = 23 °C on mannequin eye at various relative humidities from Figure 5 in terms of $\Delta C/J_E$ versus $v^{-\beta}$ for β = 0.8 and α = 6.39 (s/cm)$^{0.2}$. Data are presented as mean ± SD.

6 clearly reveals a single straight-line relationship between $\Delta C/J_E$ and $v^{-\beta}$ for all relative humidities, confirming the evaporation behavior demanded by eqs 1–3 and giving α = 6.39 (s/cm)$^{0.2}$. Noteworthy is the zero intercept in Figure 6 consistent with the absence of a lipid tear film on the mannequin eye (i.e., R_L = 0). Importantly, measurements at differing relative humidities all collapse onto a single straight line, again demanded by eqs 1–3.

These results satisfy evaporimeter criteria 1 and 2. They also mean that once the air-environment mass-transfer resistance (i.e., $R_m = \alpha v^{-\beta}$) is measured on the mannequin eye as a function of air flow, the resistance of the TFLL on human subjects, R_L, can be ascertained from eq 3 assuming that the environmental mass-transfer resistance is the same as that of the mannequin eye. We assert that the flow evaporimeter provides quantitative assessment of the TFLL in controlling tear evaporation.

3. EXPERIMENTAL PROTOCOL

3.1. Subjects. A limited pilot study of a small sample size was conducted to establish the feasibility of safe and comfortable measurement of human-tear evaporation rates with the flow evaporimeter. Three healthy male subjects (25.6 ± 6.4 years old) with no signs or symptoms of dry eye or other anterior-segment diseases were recruited from the University of California, Berkeley (UCB). Subjects had no history of contact-lens wear and were free of seasonal allergies and systemic medication. All subjects signed the informed consent form (CPHS No. 2013-03-5115) at the beginning of their first visit. This study observed the tenets of the Declaration of Helsinki and was approved by the UCB Committee for Protection of Human Subjects. Each subject was examined by a licensed optometrist at the Clinical Research Center at the School of Optometry, UCB, before and after the flow-evaporimeter validation study at each visit. Standard clinical examinations of vision and the ocular surface (e.g., cornea, conjunctiva, tear film, and adnexa) were performed using high-contrast Snellen charts and a slit lamp biomicroscope, respectively.

3.2. Investigation Protocol. Subjects came to the research facility on 15 different occasions. At each visit, the tear-evaporation rate was measured with the evaporimeter between the hours of 2 and 4 pm. Each subject visited at approximately the same time of day and within the same time period following

awakening (7−9 h). To ensure identical conditions, all measurements were conducted on weekdays, and subjects were asked to conduct only their regular activities before measurement. Prior to each tear-evaporation measurement, subjects were required to sit in an air-conditioned room (~23 °C) to acclimate for a minimum of 15 min. Subjects were subsequently asked to attach the flow-evaporimeter goggle while in a sitting position with their chins and foreheads resting on a slit-lamp support. Once the goggle housing of the flow evaporimeter was placed on the eye, gentle air flow of known flow rate and relative humidity commenced, and inlet and exit air humidity and temperature were recorded over time. Each subject undertook three measurements in a single day with a washout period of a minimum 30 min between measurements.

At commencement of the first evaporation measurement, three digital images of the studied eye were recorded to calculate the exposed palpebral and skin surface areas, A_E and A_{skin}. Eye and skin areas within the goggle were determined via a pixel-counting method adapted from Koushan et al.[81] A digital camera (Sony Cyber-Shot DSCH50, Tokyo, Japan) was used to capture three pictures of each subject (or the mannequin eye) in the primary (perpendicular) gaze position. While in a sitting position, the subject was asked to look straight ahead in a relaxed manner during photographing. A US 1-cent coin (diameter = 19.05 mm) was placed in the plane of the eye for magnification calibration. Digital images were subsequently processed with Adobe Photoshop CS5.5 (Adobe Systems Inc., San Jose, CA, USA). The region under the goggle was identified by the light pink mark left after goggle wear. Pixels of the eye and skin area under the goggle were then determined. The pixel-size calibration permitted calculation of the surface areas of the eye and skin. Average exposed ocular surface area from the three separate images was used for later calculation of evaporation flux.

Figure 7 shows a typical raw result of humidity versus time for a human subject (red line). The inlet relative humidity is 40% and the flow velocity is 5 cm/s, corresponding to a lightly ventilated room. Approximate velocities for sitting, walking, and bicycling are 10, 100, and 1000 cm/s, respectively.[82] When the eye is open, evaporimeter exit relative humidity rises to a steady value of approximately 67% within 1.5 min of goggle-evaporimeter wear. Measured exit relative humidity gauges the evaporation rate from the eye and skin exposed in the goggle. After about 5 min of wear, the subject closes both eyes. Accordingly, relative humidity in Figure 7 falls to a lower steady value corresponding to evaporation from skin alone. Tear-evaporation rates are calculated according to eq 5 from the steady plateaus in Figure 7 for open and closed eyes. The difference between open-eye and closed-eye evaporation rates gives the evaporation rate of the tears according to eq 6. For each trial, the inlet flow rate ranges from 5 to 25 cm/s for each of two relative humidities (20 and 40%) following a predetermined randomization scheme. The chosen flow-rate range reflects common indoor conditions.[83] Subjects are asked to blink normally, to look toward the farthest end of the evaporimeter inner cylinder, but not to stare. Evaporimeter-exposure time depended on the corresponding time to reach the steady exit humidity, but was limited to no more than 20 min. No discomfort was reported by subjects during or after measurement for all air flow rates and relative humidities.

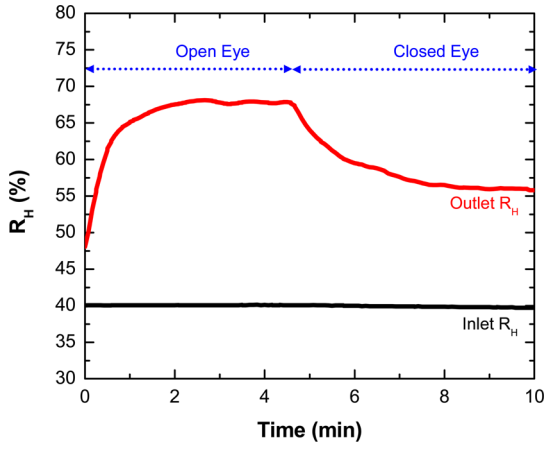

Figure 7. Typical exit relative-humidity history from the flow evaporimeter for a human subject at T_S = 35 °C (red line). The inlet flow rate is 5 cm/s. During open eye, the exit relative humidity rises, followed by a decline during closed eye. A black line gives the inlet relative humidity.

4. RESULTS AND DISCUSSION

Average tear-film evaporation rates for the three human subjects from the flow evaporimeter are shown in Figure 8 at various inlet velocities and various relative humidifies. Error bars on the data give standard error for the average of the three subjects each with three separate visits. Measured evaporation rates at low air velocity (5 cm/s) are around 2.9 × 10^{-6} and 2.2 × 10^{-6} g/cm^2/s at R_H = 20 and 40%, respectively, in accord with previously reported values.[50,77,78] Results in Figure 8 indicate considerable promise for the flow evaporimeter, (coined the Berkeley Flow Evaporimeter) to serve as a reliable and quantitative clinical tool which is comfortable, safe, and simple to operate.

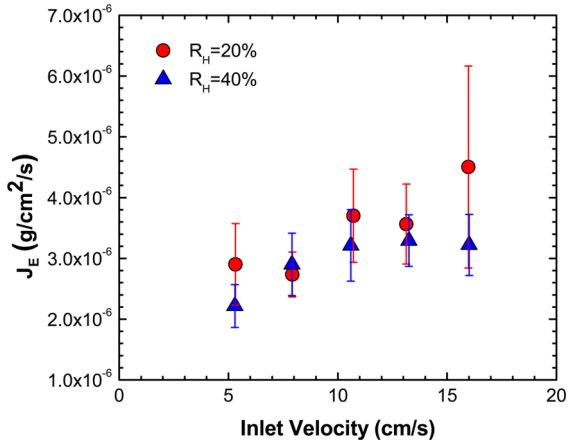

Figure 8. Evaporation rate of human subjects at T_S = 35 °C as a function of air velocity for two relative humidities. Data are presented as mean ± standard error (n = 3).

Tear-film evaporation rates in Figure 8 increase slightly at lower relative humidity and higher air velocity. However, these effects are considerably less significant compared to those of the pure-water evaporation rate measured from the mannequin model eye in Figure 5. The likely explanation is the considerable evaporation resistance of the TFLL on humans not present on the mannequin eye.

Figure 9 replots the tear-film evaporation flux from the human subjects in Figure 8, but now reported in terms of eq 3.

dx.doi.org/10.1021/ie5030497 | Ind. Eng. Chem. Res. 2014, 53, 18130−18139

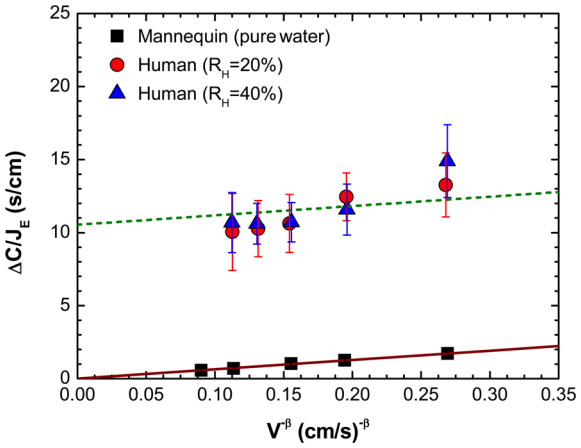

Figure 9. Average evaporimeter-determined mass-transfer resistances at T_S = 23 °C on human subjects at relative humidities of 20 and 40% in terms of $\Delta C/J_E$ versus $v^{-\beta}$ for β = 0.8. Results for the mannequin (pure water) are averaged from the relative humidities shown in Figure 6. A dashed line indicates linear fitting with a fixed slope of 6.39 (s/cm)$^{0.2}$ giving a best-fit intercept of 10.53 ± 0.63 s/cm. Data are presented as mean ± standard error (n = 3 for human subjects).

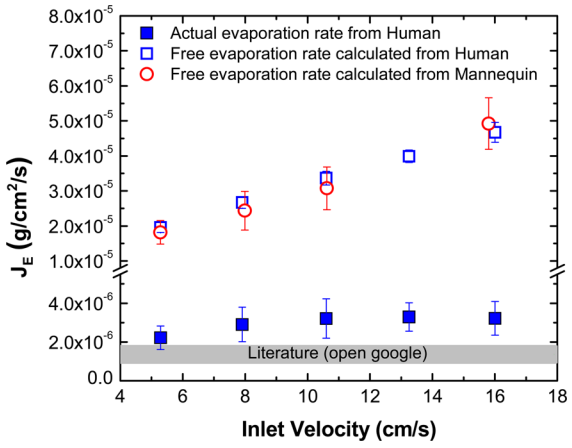

Figure 10. Comparison of estimated lipid-free evaporation rates at T_S = 35 °C (no lipid layer and R_L = 0, open symbols) from the actual measurements of human subjects (solid symbols) and from the mannequin eye (Figure 5) at various air inlet velocities at R_H = 40%. Horizontal shaded region represents the previously reported literature value for tear evaporation rate ((1.36 ± 0.65) × 10^{-6} g/cm^2/s).[50]

If we assume the air-flow profile in the goggle of the evaporimeter is identical for human eye and mannequin eye, the environmental mass-transfer resistance, R_m, for human subjects should be the same as that previously obtained from mannequin eye (i.e., α = 6.39 (s/cm)$^{0.2}$ and β = 0.8) . Figure 9 again reveals a single straight-line relationship between $\Delta C/J_E$ and $v^{-\beta}$ from human subjects, confirming the evaporation behavior demanded by eqs 1−3. Moreover, measurements at different relative humidities collapse onto a single straight line (dashed) parallel to that from the mannequin eye. This result validates our assumption that R_m for human subjects is identical to that obtained from the mannequin model eye. (i.e., the air-phase mass-transfer resistance of the evaporimeter depends primarily on instrument design and not strongly on the particular eye under study). Based on eq 3, the intercept of this line for human subjects in Figure 9 is the TFLL mass-transfer resistance R_L (10.54 ± 0.63 s/cm). Upon assuming an average TFLL thickness of 100 nm,[26] the water diffusion permeability in TFLL is thus estimated by eq 4 as 0.95 × 10^{-10} m^2/s in agreement with our previous estimation based on clinical observation on evaporation rate reduction due to lipid layer deficiency.[33] Quantitative extraction of human-TFLL resistance from measured flow-evaporimeter data suggests that R_L is not a strong function of air flow or relative humidity. We find that the Berkeley Flow Evaporimeter successfully garners TFLL resistance.

Figure 10 plots the average tear-evaporation flux of the three human subjects at T_S = 35 °C (filled squares) as a function of air-flow velocity at 40% relative humidity compared to corresponding calculated lipid-free water evaporation rates at T_S = 35 °C (open squares). Open squares in Figure 10 are calculated from the human-subject data after eliminating the TFLL resistance. By setting R_L = 10.53 s/cm (see Figure 9), the environment-air resistance, R_m, from each human-subject evaporation rate (filled squares) is determined from eq 3, and subsequently used to calculate the "lipid-free" tear-film evaporation rate (where no TFLL exists and R_L = 0) with eq 1. Note the scale change of the ordinate. Calculated lipid-free water evaporation rates at T_S = 35 °C (open squares) are approximately an order of magnitude larger than those from human tear with a TFLL (filled squares). Figure 10 clearly indicates that the lipid-free water evaporation rate (no TFLL) also strongly depends on air velocity. For example, at an inlet air velocity of around 10 cm/s, which represents sitting in a typical ventilated room, the lipid-free tear-film evaporation rate (no TFLL) is 10-fold higher than the human tear-film evaporation rate. This finding accentuates the importance of the TFLL resistance in controlling human-tear evaporation. It is also in excellent agreement with the current clinical assumption that TFLL reduces tear-film evaporation rates by up to 90%.[27,28] The shaded region in Figure 10 reports the literature value for human subjects ((1.36 ± 0.65) × 10^{-6} g/cm^2/s).[50] Our evaporimeter gives similar results, but in addition, allows evaluation of human TFLL resistance.

To confirm further that the environmental mass-transfer resistance, R_m, measured on the mannequin eye (with no TFLL and at ∼23 °C) applies to human subjects, we calculated the pure-water evaporation rate from eq 1 at human-eye temperature (T_S = 35 °C) using α and β determined from Figure 6. This calculation is shown as open circles in Figure 10. Lipid-free evaporation rates estimated from both human and mannequin eyes directly overlap. This exercise confirms that the environmental air resistance parameters α and β depend only weakly on temperature. It also strongly suggests that evaporation rates from a "lipid-free" human tear film are equivalent to those from a pure-water film. More importantly, we validate that the Berkeley Flow Evaporimeter obeys the dissolution/evaporation picture of Figure 1 as embodied in eqs 1−3.

Figure 11 shows the tear-film evaporation rate plotted in terms of eq 3 from each separate human subject in this study. Slopes of the fit dashed lines are fixed by setting the environmental air resistance equal to that obtained from mannequin eye, as shown in Figure 9. With this restriction, best-fit intercepts give the TFLL layer resistance of each human subject. Subject description and individual fitted R_L values are summarized in Table 1. Our prototype flow evaporimeter clearly assesses differences in the TFLL mass-transfer resistance among subjects due to, for example, the variation in TFLL thickness and/or in composition by age, race/ethnicity, gender, etc. With human subjects, R_L is a dynamic parameter controlled

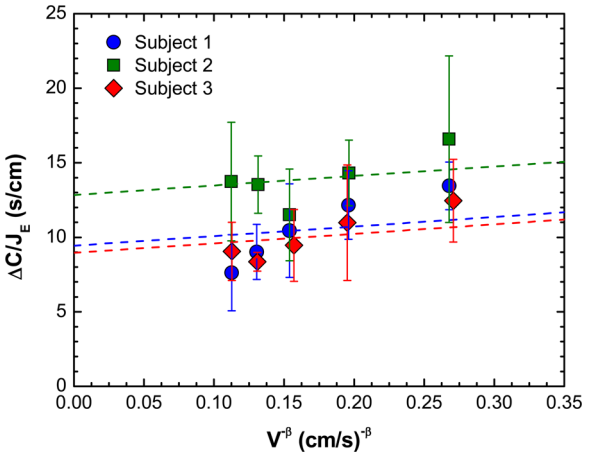

Figure 11. Individual evaporimeter-determined mass-transfer resistance results on human subjects in terms of $\Delta C/J_E$ versus $v^{-\beta}$ for β = 0.8. Dashed lines indicate linear fitting with a fixed slope of 6.39 characteristic of the mannequin eye. Description of subjects and the respective fitted intercepts giving R_L are summarized in Table 1. Data are presented as mean ± SD (n = 6, three for R_H = 20% and three for R_H = 40%).

Table 1. Measured TFLL Mass-Transfer Resistance (R_L) from Human Subjects

subject	age (years)	race	sex	R_L,[a] s/cm
1	21	Caucasian	male	9.44 ± 0.88
2	33	Asian	male	12.84 ± 0.69
3	22	Caucasian	male	8.95 ± 0.56

[a]Mean ± standard error.

not only by the intrinsic factors, such as age, gender, diet, race, etc., but also by extrinsic factors, such as harsh environmental conditions (dry, windy), contact-lens wear, blink rate, and physical activities (running, bicycling). Changes in the lipid thickness and composition might also vary with the time of the day.

Because best-fit slopes in Figures 9 and 11 are not precisely those corresponding to the mannequin eye, especially for subject 1, it is possible that R_m varies between individuals. Differences in environmental mass resistance, R_m, between the mannequin and the human subjects might be due to differences in eye-cavity shapes and blinking patterns for each subject. Nevertheless, to our knowledge, our effort is the only pilot study to quantify in vivo mass-transfer resistances of the TFLL. The Berkeley Flow Evaporimeter lays a foundation for more extensive clinical studies to evaluate interrelationships among primary physiological variables and tear-film evaporation rates.

Human-subject behavior is variable, requiring large sample sizes to characterize statistically meaningful averages. Thus, a larger clinical sample size is requisite to establish the repeatability and reproducibility of in vivo evaporation-rate measurement by the flow evaporimeter. Our initial human-subject pilot study, although very limited, demonstrates the feasibility of the Berkeley Flow Evaporimeter to serve as a reliable and quantitative clinical tool for quantifying tear-film evaporation rates.

5. CONCLUSIONS

Lack of a precise, inexpensive, and easy-to-use diagnostic tool prevents optometry clinicians from employing tear-film evaporation rate as simple diagnostic for dry eye. Current devices for measuring tear-evaporation rate incompletely account for evaporation rates varying strongly with air flow and relatively humidity in the surrounding environment, thereby yielding inconclusive and suspect results. We developed a novel flow evaporimeter that accounts for the physical factors known to affect the evaporation rate including air flow, temperature, and humidity and, thus, provides quantitative measurement of in vivo tear-evaporation rates.

Our flow evaporimeter supplies a well-defined flow field to the eye with known and adjustable flow rates and relative humidities, and yields repeatable and accurate evaporation rates for pure water. Environment mass-transfer resistances are quantified for the flow evaporimeter allowing the mass-transfer resistance of the human tear-film lipid layer to be established without the need for an environmental chamber. The flow evaporimeter provides its own environmental conditions. Preliminary in vivo studies on three human subjects validates the feasibility of the flow evaporimeter to obtain tear-film evaporation rates and confirms the additive mass-transfer resistances based on the dissolution/evaporation mechanism undergirding the design of the flow evaporimeter. This is the first work that identifies the mass-transfer resistance from the lipid layer covering human eyes. The Berkeley Flow Evaporimeter is an accurate, safe, and convenient diagnostic tool that meets the requisite design criteria and is suitable for clinical evaluation of dry-eye-related maladies.

AUTHOR INFORMATION

Corresponding Author

*E-mail: radke@berkeley.edu. Tel.: (510) 642-5204. Fax: (510) 642-4778.

Notes

The authors declare no competing financial interest.

ACKNOWLEDGMENTS

The authors thank the volunteer subjects for participating in the flow-evaporimeter validation study.

REFERENCES

(1) Viso, E.; Rodriguez-Ares, M. T.; Gude, F. Prevalence of and associated factors for dry eye in a spanish adult population (the salnes eye study). *Ophthalmic Epidemiol.* **2009**, *16* (1), 15−21.

(2) Versura, P.; Cellini, M.; Torreggiani, A.; Profazio, V.; Bernabini, B.; Caramazza, R. Dryness symptoms, diagnostic protocol and therapeutic management: A report on 1,200 patients. *Ophthalmic Res.* **2001**, *33* (4), 221−227.

(3) Tongg, L.; Saw, S.-M.; Lamoureux, E. L.; Wang, J. J.; Rosman, M.; Tan, D. T.; Wong, T. Y. A questionnaire-based assessment of symptoms associated with tear film dysfunction and lid margin disease in an asian population. *Ophthalmic Epidemiol.* **2009**, *16* (1), 31−37.

(4) Uchino, M.; Dogru, M.; Yagi, Y.; Goto, E.; Tomita, M.; Kon, T.; Saiki, M.; Matsumoto, Y.; Uchino, Y.; Yokoi, N. The features of dry eye disease in a japanese elderly population. *Optom. Vision Sci.* **2006**, *83* (11), 797−802.

(5) Lin, P.-Y.; Cheng, C.-Y.; Hsu, W.-M.; Tsai, S.-Y.; Lin, M.-W.; Liu, J.-H.; Chou, P. Association between symptoms and signs of dry eye among an elderly chinese population in taiwan: The shihpai eye study. *Invest. Ophthalmol. Visual Sci.* **2005**, *46* (5), 1593−1598.

(6) Schaumberg, D. A.; Sullivan, D. A.; Buring, J. E.; Dana, M. R. Prevalence of dry eye syndrome among US women. *Am. J. Ophthalmol.* **2003**, *136* (2), 318−326.

(7) Uchiyama, E.; Aronowicz, J. D.; Butovich, I. A.; McCulley, J. P. Increased evaporative rates in laboratory testing conditions simulating

airplane cabin relative humidity: An important factor for dry eye syndrome. *Eye Contact Lens* **2007**, *33* (4), 174−176.
(8) McCulley, J. P.; Aronowicz, J. D.; Uchiyama, E.; Shine, W. E.; Butovich, I. A. Correlations in a change in aqueous tear evaporation with a change in relative humidity and the impact. *Am. J. Ophthalmol.* **2006**, *141* (4), 758−760.
(9) Guillon, M.; Maïssa, C. Tear film evaporation—effect of age and gender. *Contact Lens Anterior Eye* **2010**, *33* (4), 171−175.
(10) Abusharha, A. A.; Pearce, E. I. The effect of low humidity on the human tear film. *Cornea* **2013**, *32* (4), 429−434.
(11) The epidemiology of dry eye disease: Report of the epidemiology subcommittee of the international dry eye workshop (2007). *Ocul. Surf.* **2007**, *5*, (2), 93−107.
(12) Gayton, J. L. Etiology, prevalence, and treatment of dry eye disease. *Clin. Ophthalmol.* **2009**, *3*, 405−412.
(13) Schaumberg, D.; Sullivan, D.; Dana, M. R. Epidemiology of dry eye syndrome. In *Lacrimal Gland, Tear Film, and Dry Eye Syndromes 3*; Sullivan, D., Stern, M., Tsubota, K., Dartt, D., Sullivan, R., Bromberg, B. B., Eds.; Advances in Experimental Medicine and Biology 506; Springer: New York, 2002; pp 989−998.
(14) O'Brien, P. D.; Collum, L. M. Dry eye: Diagnosis and current treatment strategies. *Curr. Allergy Asthma Rep.* **2004**, *4* (4), 314−319.
(15) Lemp, M. A.; Baudouin, C.; Baum, J.; Dogru, M.; Foulks, G. N.; Kinoshita, S.; Laibson, P.; McCulley, J.; Murube, J.; Pflugfelder, S. C.; Rolando, M.; Toda, I. The definition and classification of dry eye disease: Report of the definition and classification subcommittee of the international dry eye workshop. *Ocul. Surf.* **2007**, *5* (2), 75−92.
(16) Gaffney, E.; Tiffany, J.; Yokoi, N.; Bron, A. A mass and solute balance model for tear volume and osmolarity in the normal and the dry eye. *Prog. Retinal Eye Res.* **2010**, *29* (1), 59−78.
(17) Cerretani, C. F.; Radke, C. Tear dynamics in healthy and dry eyes. *Curr. Eye Res.* **2014**, *39* (6), 1−16.
(18) Baudouin, C. The pathology of dry eye. *Surv. Ophthalmol.* **2001**, *45*, S211−S220.
(19) Bron, A. J.; Yokoi, N.; Gaffney, E.; Tiffany, J. M. Predicted phenotypes of dry eye: Proposed consequences of its natural history. *Ocul. Surf.* **2009**, *7* (2), 78−92.
(20) Hirata, H.; Meng, I. D. Cold-sensitive corneal afferents respond to a variety of ocular stimuli central to tear production: Implications for dry eye disease. *Invest. Ophthalmol. Visual Sci.* **2010**, *51* (8), 3969−3976.
(21) Wong, H.; Fatt, I.; Radke, C. J. Deposition and thinning of the human tear film. *J. Colloid Interface Sci.* **1996**, *184* (1), 44−51.
(22) Creech, J. L.; Do, L. T.; Fatt, I.; Radke, C. J. In vivo tear-film thickness determination and implications for tear-film stability. *Curr. Eye Res.* **1998**, *17* (11), 1058−1066.
(23) King-Smith, E.; Fink, B.; Hill, R.; Koelling, K.; Tiffany, J. The thickness of the tear film. *Curr. Eye Res.* **2004**, *29* (4−5), 357−368.
(24) Craig, J. Structure and function of the preocular tear film. In *The Tear Film: Structure, Function and Clinical Examination*; Butterworth-Heinemann Medical: Woburn, MA, 2002; pp 18−50.
(25) Rosenfeld, L.; Cerretani, C.; Leiske, D. L.; Toney, M. F.; Radke, C. J.; Fuller, G. G. Structural and rheological properties of meibomian lipid. *Invest. Ophthalmol. Visual Sci.* **2013**, *54* (4), 2720−2732.
(26) Mishima, S. Some physiological aspects of the precorneal tear film. *Arch. Ophthalmol.* **1965**, *73* (2), 233−241.
(27) Craig, J. P.; Tomlinson, A. Importance of the lipid layer in human tear film stability and evaporation. *Optom. Vision Sci.* **1997**, *74* (1), 8−13.
(28) Mishima, S.; Maurice, D. M. The oily layer of the tear film and evaporation from the corneal surface. *Exp. Eye Res.* **1961**, *1* (1), 39−45.
(29) Wolff, E.; Last, R. J. *Anatomy of the Eye and Orbit, Including the Central Connections, Development, and Comparative Anatomy of the Visual Apparatus*; Saunders: Philadelphia, 1961.
(30) King-Smith, P. E.; Nichols, J. J.; Braun, R. J.; Nichols, K. K. High resolution microscopy of the lipid layer of the tear film. *Ocul. Surf.* **2011**, *9* (4), 197−211.
(31) Kimball, S. H.; King-Smith, P. E.; Nichols, J. J. Evidence for the major contribution of evaporation to tear film thinning between blinks. *Invest. Ophthalmol. Visual Sci.* **2010**, *51* (12), 6294−6297.
(32) King-Smith, P. E.; Hinel, E. A.; Nichols, J. J. Application of a novel interferometric method to investigate the relation between lipid layer thickness and tear film thinning. *Invest. Ophthalmol. Visual Sci.* **2010**, *51* (5), 2418−2423.
(33) Peng, C.-C.; Cerretani, C.; Braun, R. J.; Radke, C. J. Evaporation-driven instability of the precorneal tear film. *Adv. Colloid Interface Sci.* **2014**, *206*, 250−264.
(34) Cerretani, C. F.; Ho, N. H.; Radke, C. J. Water-evaporation reduction by duplex films: Application to the human tear film. *Adv. Colloid Interface Sci.* **2013**, *197−198*, 33−57.
(35) Fonn, D. Targeting contact lens induced dryness and discomfort: What properties will make lenses more comfortable. *Optom. Vision Sci.* **2007**, *84* (4), 279−285.
(36) Hamano, H.; Hori, M.; Kawabe, H.; Mitsunaga, S.; Ohnishi, Y.; Koma, I. Modification of the superficial layer of the tear film by the secretion of the meibomian glands. *Folia Ophthalmol. Jpn.* **1980**, *31*, 353−360.
(37) Rolando, M.; Refojo, M. F. Tear evaporimeter for measuring water evaporation rate from the tear film under controlled conditions in humans. *Exp. Eye Res.* **1983**, *36* (1), 25−33.
(38) Rolando, M.; Refojo, M. F.; Kenyon, K. R. Increased tear evaporation in eyes with keratoconjunctivitis sicca. *Arch. Ophthalmol.* **1983**, *101* (4), 557−558.
(39) Trees, G. R.; Tomlinson, A. Effect of artificial tear solutions and saline on tear film evaporation. *Optom. Vision Sci.* **1990**, *67* (12), 886−890.
(40) Tomlinson, A.; Trees, G. R. Effect of preservatives in artificial tear solutions on tear film evaporation. *Ophthalmic Physiol. Opt.* **1991**, *11* (1), 48−52.
(41) Tomlinson, A.; Trees, G. R.; Occhipinti, J. R. Tear production and evaporation in the normal eye. *Ophthalmic Physiol. Opt.* **1991**, *11* (1), 44−47.
(42) Tsubota, K.; Yamada, M. Tear evaporation from the ocular surface. *Invest. Ophthalmol. Visual Sci.* **1992**, *33* (10), 2942−2950.
(43) Mathers, W. D. Ocular evaporation in meibomian gland dysfunction and dry eye. *Ophthalmology* **1993**, *100* (3), 347−351.
(44) Mathers, W. D.; Binarao, G.; Petroll, M. Ocular water evaporation and the dry eye: A new measuring device. *Cornea* **1993**, *12* (4), 335−340.
(45) Mathers, W. D.; Daley, T. E. Tear flow and evaporation in patients with and without dry eye. *Ophthalmology* **1996**, *103* (4), 664−669.
(46) Mathers, W. D.; Lane, J. A. Meibomian gland lipid, evaporation, and tear film stability. In *Lacrimal Gland, Tear Film, and Dry Eye Syndromes 2*; Sullivan, D. A., Ed.; Plenum: New York, 1998; pp 349−360.
(47) Craig, J. P.; Singh, I.; Tomlinson, A.; Morgan, P. B.; Efron, N. The role of tear physiology in ocular surface temperature. *Eye* **2000**, *14* (4), 635−641.
(48) Goto, E.; Endo, K.; Suzuki, A.; Fujikura, Y.; Matsumoto, Y.; Tsubota, K. Tear evaporation dynamics in normal subjects and subjects with obstructive meibomian gland dysfunction. *Invest. Ophthalmol. Visual Sci.* **2003**, *44* (2), 533−539.
(49) McCulley, J. P.; Shine, W. E.; Aronowicz, J.; Oral, D.; Vargas, J. Presumed hyposecretory/hyperevaporative KCS: Tear characteristics. *Trans. Am. Ophthalmol. Soc.* **2003**, *101*, 141−154.
(50) Mathers, W. Evaporation from the ocular surface. *Exp. Eye Res.* **2004**, *78* (3), 389−394.
(51) McCulley, J. P.; Uchiyama, E.; Aronowicz, J. D.; Butovich, I. A. Impact of evaporation on aqueous tear loss. *Trans. Am. Ophthalmol. Soc.* **2006**, *104*, 121−128.
(52) Guillon, M.; Maissa, C. Contact lens wear affects tear film evaporation. *Eye Contact Lens* **2008**, *34* (6), 326−330.
(53) Wojtowicz, J. C.; McCulley, J. P. Assessment and impact of the time of day on aqueous tear evaporation in normal subjects. *Eye Contact Lens* **2009**, *35* (3), 117−119.

(54) Madden, L. C.; Tomlinson, A.; Simmons, P. A. Effect of humidity variations in a controlled environment chamber on tear evaporation after dry eye therapy. *Eye Contact Lens* **2013**, *39* (2), 169−174.
(55) Rohit, A.; Brown, S.; Willcox, M. D. P.; Stapleton, F. The effect of tear lipid biochemistry on tear evaporation rate during contact lens wear. *Invest. Ophthalmol. Visual Sci.* **2013**, *54*, E-abstract 4358.
(56) Cedarstaff, T.; Tomlinson, A. A comparative study of tear evaporation rates and water content of soft contact lenses. *Am. J. Optom. Physiol. Optics* **1983**, *60* (3), 167−174.
(57) Rohit, A.; Ehrmann, K.; Naduvilath, T.; Willcox, M.; Stapleton, F. Validating a new device for measuring tear evaporation rates. *Ophthalmic Physiol. Opt.* **2014**, *34* (1), 53−62.
(58) Petznick, A.; Tan, J. H.; Boo, S. K.; Lee, S. Y.; Acharya, U. R.; Tong, L. Repeatability of a new method for measuring tear evaporation rates. *Optom. Vision Sci.* **2013**, *90* (4), 366−371.
(59) Tan, J.-H.; Ng, E.; Acharya, U. R. Evaluation of tear evaporation from ocular surface by functional infrared thermography. *Med. Phys.* **2010**, *37* (11), 6022−6034.
(60) Khanal, S.; Tomlinson, A.; McFadyen, A.; Diaper, C.; Ramaesh, K. Dry eye diagnosis. *Invest. Ophthalmol. Visual Sci.* **2008**, *49* (4), 1407−1414.
(61) Methodologies to diagnose and monitor dry eye disease: Report of the diagnostic methodology subcommittee of the international dry eye workshop (2007). *Ocul. Surf.* **2007**, *5*, (2), 108−152.
(62) Nichols, K. K.; Foulks, G. N.; Bron, A. J.; Glasgow, B. J.; Dogru, M.; Tsubota, K.; Lemp, M. A.; Sullivan, D. A. The international workshop on meibomian gland dysfunction: Executive summary. *Invest. Ophthalmol. Visual Sci.* **2011**, *52* (4), 1922−1929.
(63) Knop, E.; Knop, N.; Millar, T.; Obata, H.; Sullivan, D. A. The international workshop on meibomian gland dysfunction: Report of the subcommittee on anatomy, physiology, and pathophysiology of the meibomian gland. *Invest. Ophthalmol. Visual Sci.* **2011**, *52* (4), 1938−1978.
(64) Craig, J. P.; Willcox, M. D.; Argüeso, P.; Maissa, C.; Stahl, U.; Tomlinson, A.; Wang, J.; Yokoi, N.; Stapleton, F. The TFOS international workshop on contact lens discomfort: Report of the contact lens interactions with the tear film subcommittee. *Invest. Ophthalmol. Visual Sci.* **2013**, *54* (11), TFOS123−TFOS156.
(65) Saettone, M. F. Progress and problems in ophthalmic drug delivery. *Business Briefing: Pharmatech*; World Markets Research Centre: London, 2002; pp 1−6.
(66) Vasir, J. K.; Tambwekar, K.; Garg, S. Bioadhesive microspheres as a controlled drug delivery system. *Int. J. Pharm.* **2003**, *255* (1), 13−32.
(67) Bird, R. B.; Stewart, W. E.; Lightfoot, E. N. *Transport Phenomena*, revised 2nd ed.; John Wiley & Sons, Inc.: New York, 2007.
(68) Hart, D. E.; Simko, M.; Harris, E. How to produce moisture chamber eyeglasses for the dry eye patient. *J. Am. Optom. Assoc.* **1994**, *65* (7), 517−522.
(69) Li, L.; Braun, R. J. A model for the human tear film with heating from within the eye. *Phys. Fluids* **2012**, *24* (6), 062103.
(70) Braun, R. J. Dynamics of the tear film. *Annu. Rev. Fluid Mech.* **2012**, *44*, 267−297.
(71) Chhabra, M.; Prausnitz, J. M.; Radke, C. J. A single-lens polarographic measurement of oxygen permeability (*Dk*) for hyper-transmissible soft contact lenses. *Biomaterials* **2007**, *28* (30), 4331−4342.
(72) Chin, D. T.; Tsang, C. H. Mass transfer to an impinging jet electrode. *J. Electrochem. Soc.* **1978**, *125*, 1461−1470.
(73) Hoch, G.; Chauhan, A.; Radke, C. Permeability and diffusivity for water transport through hydrogel membranes. *J. Membr. Sci.* **2003**, *214* (2), 199−209.
(74) Fornasiero, F.; Krull, F.; Prausnitz, J. M.; Radke, C. J. Steady-state diffusion of water through soft-contact-lens materials. *Biomaterials* **2005**, *26* (28), 5704−5716.
(75) Tiffany, J. M.; Todd, B. S.; Baker, M. R. Computer-assisted calculation of exposed area of the human eye. In *Lacrimal Gland, Tear Film, and Dry Eye Syndromes 2*; Sullivan, D. A., Ed.; Plenum: New York, 1998; pp 433−439.
(76) Roth, T.; Loncin, M. Evaluation of water evaporation inhibitors. *J. Colloid Iinterface Sci.* **1984**, *100* (1), 216−219.
(77) King-Smith, P. E.; Nichols, J. J.; Nichols, K. K.; Fink, B. A.; Braun, R. J. Contributions of evaporation and other mechanisms to tear film thinning and break-up. *Optom. Vision Sci.* **2008**, *85* (8), 623−630.
(78) Tomlinson, A.; Doane, M. G.; McFadyen, A. Inputs and outputs of the lacrimal system: Review of production and evaporative loss. *Ocul. Surf.* **2009**, *7* (4), 186−198.
(79) Hisatake, K.; Tanaka, S.; Aizawa, Y. Evaporation rate of water in a vessel. *J. Appl. Phys.* **1993**, *73* (11), 7395−7401.
(80) Hisatake, K.; Fukuda, M.; Kimura, J.; Maeda, M.; Fukuda, Y. Experimental and theoretical study of evaporation of water in a vessel. *J. Appl. Phys.* **1995**, *77* (12), 6664−6674.
(81) Koushan, K.; Skibell, B. C.; Harvey, J. T.; Jankowski, H. K.; Deangelis, D. D.; Oestreicher, J. H. Digital photography as a novel technique of measuring ocular surface dimensions. *Orbit* **2008**, *27* (4), 259−265.
(82) Fornasiero, F.; Prausnitz, J. M.; Radke, C. J. Post-lens tear-film depletion due to evaporative dehydration of a soft contact lens. *J. Membr. Sci.* **2006**, *275* (1), 229−243.
(83) Baldwin, P. E. J.; Maynard, A. D. A survey of wind speeds in indoor workplaces. *Ann. Occup. Hyg.* **1998**, *42* (5), 303−313.